A new approach to increasing the efficiency of low-pH Fe-electrocoagulation applications

Youri Gendel*, Ori Lahav

Faculty of Civil and Environmental Engineering, Technion, Haifa, 32000, Israel

ABSTRACT

Incomplete oxidation of Fe(II) species released from the anode to Fe(III) may impede iron electrocoagulation processes conducted under low dissolved oxygen and/or pH < 7 conditions, accompanied by the typically high buffering capacity of wastewater. This paper introduces a new approach to overcome this drawback by applying a second electrochemical cell (Ti/RuO$_2$ anode and Ti cathode) to be operated in parallel to the electrocoagulation cell. The second unit oxidizes Cl$^-$ ions invariably present in the water to HOCl, which is capable of oxidizing Fe(II) species at a high rate, irrespective of pH or O$_{2(aq)}$ concentration. An electrolytic cell with a Ti/RuO$_2$ anode and Ti cathode was shown to successively operate in parallel to a sacrificial electrocoagulation cell (Fe anode and Ti cathode) to attain complete Fe(II) conversion to Fe(III) under low-pH conditions, in which, in the absence of the 2nd cell, unwanted Fe(II) species would have dominated the dissolved iron species. Current efficiency for Cl$_2$ production was 12.4% and 45.7% at 200 and 1000 mg Cl/l, respectively. Under three practical conditions (pH 6, [Cl$^-$] = 200 mg/l; pH 6, [Cl$^-$] = 400 mg/l; pH 5, [Cl$^-$] = 600 mg/l) the power demand of the combined system was 25.29, 12.7 and 8.1 kWh/kg Fe(III)$_{produced}$, respectively, suggesting that the presented approach is competitive at [Cl$^-$] > ~600 mg/l.

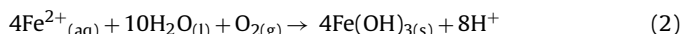© 2010 Elsevier B.V. All rights reserved.

1. Introduction

Electrocoagulation (EC) using sacrificial iron anodes has been extensively investigated for the removal of suspended solids, organic species, color, metal ions, inorganic anions and a variety of other constituents in water and wastewater [1–4]. Iron hydroxide species, formed as a result of the electrochemical Fe anode dissolution and subsequent Fe(II) species oxidation, are positively charged thereby have the potential to destabilize negatively charged suspended particles, resulting in aggregation and floc formation. At higher iron dosages coagulation typically occurs through the mechanism of sweep flocculation [1,5]. The almost exclusive *in situ* product of Fe anode dissolution has been shown to be Fe(II) [5,6]. According to solution pH and the dissolved oxygen concentration Fe(II) species can be potentially oxidized to the Fe(III) form, which is usually the main active species in either coagulation pathway.

Two mechanism pathways (Eqs. (1)–(8)) have been proposed to describe the generation of iron-hydroxide species in electrocoagulation processes [7].
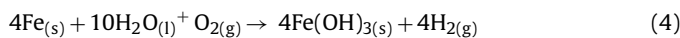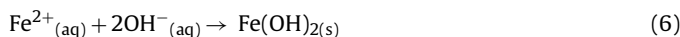
1.1. Mechanism 1

Anode:

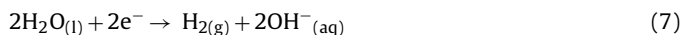$$4Fe_{(s)} \rightarrow 4Fe^{2+}_{(aq)} + 8e^- \tag{1}$$

$$4Fe^{2+}_{(aq)} + 10H_2O_{(l)} + O_{2(g)} \rightarrow 4Fe(OH)_{3(s)} + 8H^+ \tag{2}$$

Cathode:

$$8H^+_{(aq)} + 8e^- \rightarrow 4H_{2(g)} \tag{3}$$

Overall:

$$4Fe_{(s)} + 10H_2O_{(l)}{}^+ O_{2(g)} \rightarrow 4Fe(OH)_{3(s)} + 4H_{2(g)} \tag{4}$$

1.2. Mechanism 2

Anode:

$$Fe_{(s)} \rightarrow Fe^{2+}_{(aq)} + 2e^- \tag{5}$$

$$Fe^{2+}_{(aq)} + 2OH^-_{(aq)} \rightarrow Fe(OH)_{2(s)} \tag{6}$$

Cathode:

$$2H_2O_{(l)} + 2e^- \rightarrow H_{2(g)} + 2OH^-_{(aq)} \tag{7}$$

Overall:

$$Fe_{(s)} + 2H_2O_{(l)} \rightarrow Fe(OH)_{2(s)} + H_{2(g)} \tag{8}$$
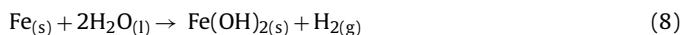
* Corresponding author. Tel.: +972 4 8292191; fax: +972 4 8228898.
E-mail addresses: ygendel@techunix.technion.ac.il, agori@technion.ac.il
(Y. Gendel).

Lakshmanan et al. [5] showed that wustite ($Fe(OH)_{2(s)}$) formation (Eq. (6)) does not occur in practice in solutions containing silica and bicarbonate ions and that wustite formation in the absence of silica and bicarbonate is possible only at pH > 8. It seems likely thus that for the majority of practical solution compositions Mechanism 1 is the dominant pathway.

Ferric iron hydroxides formed by Fe(II) oxidation (Eq. (2)) are normally the target product of iron electrocoagulation processes. However, the rate of Fe(II) oxidation is highly dependent on solution pH and to a lesser degree on the dissolved Fe(II) and oxygen concentrations and the presence of Fe(II) complexing agents [8]. Accordingly, Lakshmanan et al. [5] observed complete oxidation of Fe(II) during electrocoagulation operated at pH 8.5. At lower pH values (pH 6.5 and pH 7.5) the observed Fe(II) oxidation rate was much slower and the percentage of Fe(II) species remaining in solution were 70–85% and 10–45%, respectively (electrolysis time: 60 s, mixing time: 2 min (including the electrolysis time), current densities: 1.32–21.1 mA/cm^2). Additionally, it was shown by [5] that higher current densities at a given pH result in higher Fe(II) oxidation rates. This observation was attributed to elevated pH values that develop near the cathode due to the reduction of H$^+$ ions to H$_{2(g)}$ [5]. At the higher current densities the pH value that developed nearby the cathode was higher due to more rapid consumption of H$^+$ ions, resulting in faster Fe(II) oxidation kinetics.
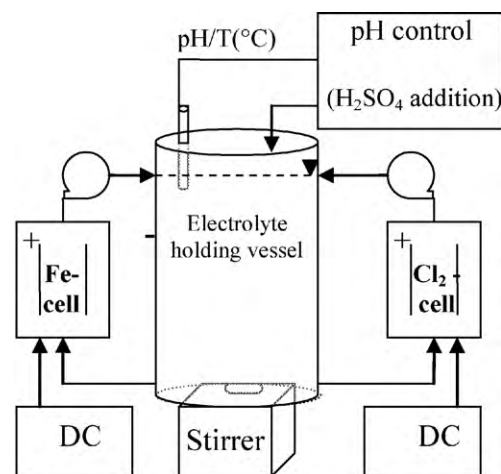
It can be thus concluded that the rate of Fe(II) oxidation in iron electrocoagulation reactors at the pH 5–pH 7 range (and thus the overall process efficiency) is highly dependent on the buffering capacity of the electrolyzed solution. In solutions with low buffering capacity the rate of H$^+$ ions consumption at the cathode may result in sufficiently high local pH values in the electrolytic cell, and thus a high Fe(II) oxidation rate can be expected even in solutions with relatively low initial pH (pH 5–pH 6.5). In contrast, in highly buffered water (or wastewater) capable of resisting the increase in pH due to the H$^+$ consumption, the conversion of Fe(II) into Fe(III) is expected to be slow, eventually resulting in a less efficient electrocoagulation process. Natural waters and wastewaters usually have a relatively high pH buffering capacity at the pH 5–pH 7 range due to the presence of (mainly) carbonate species and in wastewater also dissolved phosphate and various organic acids. Consequently, complete Fe(II) oxidation during Fe-electrocoagulation processes operated at pH < 7 (which may also be accompanied with low dissolved oxygen concentration) may be difficult to attain within the electrocoagulation process, a fact which detracts from the effectiveness of this approach in low-pH water.

To overcome the potential incomplete Fe(II) oxidation the introduction of a second electrolysis cell, consisting of a non-sacrificial anode, is proposed in this study. The second cell is operated as an integral part of the electrocoagulation system. Chloride ions, invariably present in water and wastewater at various concentrations, can be oxidized into chlorine ($Cl_{2(g)}$) on a dimensionally stable anode such as Ti/RuO$_2$ [9]. At pH > ~3 $Cl_{2(g)}$ reacts with water to form dissolved hypochlorous acid/hypochlorite ions [10]. All three active chlorine species (Cl_2, HOCl and OCl$^-$) are capable of oxidizing Fe(II) to Fe(III) at a very high rate, practically irrespective of pH [11]. The indirect electrochemical Fe(II) oxidation in the proposed second electrolysis cell is described by the following equations:
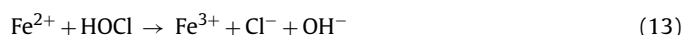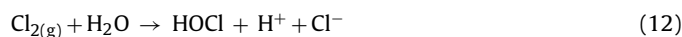
At the anode:

$$2Cl^- \rightarrow Cl_{2(g)} \tag{9}$$

$$2H_2O \rightarrow O_2 + 4H^+ + 4e^- \tag{10}$$

At the cathode:

$$2H_2O + 2e^- \rightarrow H_2 + 2OH^- \tag{11}$$

Fig. 1. Experimental setup applied in electrochemical studies. Fe-cell: electrolyzer with iron anode and Ti cathode; Cl$_2$-cell: electrolyzer with Ti/RuO$_2$ anode and Ti cathode. Electrolyte solution was recirculated between the stirred vessel and electrolysers. In the separate-cell studies either Fe-cell or Cl$_2$-cell was operated alone.

In the bulk solution

$$Cl_{2(g)} + H_2O \rightarrow HOCl + H^+ + Cl^- \tag{12}$$

$$Fe^{2+} + HOCl \rightarrow Fe^{3+} + Cl^- + OH^- \tag{13}$$

where Fe^{2+} and Fe^{3+} represent all the possible complexes that can form with Fe(II) and Fe(III) species, respectively.

O$_{2(g)}$ evolution (Eq. (10)) is expected to be the main unwanted reaction on the anode surface. The main operational parameters expected to govern the hypochlorite production efficiency at given temperature, electroyzer design and electrode material are the chloride ion concentration, the current density and the interelectrode gap [9]. Once hypochlorite is formed it is expected to react immediately with Fe(II) species. Therefore, phenomena such as formation of chlorate ions (ClO$_3$$^-$) in the bulk solution, cathodic back-reduction of HOCl to chloride and other reactions leading to loss of efficiency and that are often observed in conventional hypochlorite production electrochemical systems [12], are not expected to occur in the proposed system.

The present study is aimed to serve as a proof-of-concept for the proposed dual-cell iron electrocoagulation process. No optimization of the overall system (i.e. in order to define optimal operational regimes for the two electrochemical units at given conditions) is thus presented, but rather specific cases are analyzed. Three separate studies were carried out within this scope. First, the dissolution of a Fe anode and the consequent Fe(II) and Fe(III) formation rates were studied within a range of operational conditions (i.e. chloride ions concentration range of 200–1000 mg/l, 2 < pH < 7, varied electrolyte buffering intensity and different applied current densities). Thereafter, active chlorine production rates were obtained as a function of the electrolyte composition and applied currents. Finally, the two electrochemical units were operated together to result in (practically) full dissolution of the Fe anode directly into Fe(III) species at low-pH conditions.

2. Experimental

Electrochemical experiments were carried out using the experimental system shown in Fig. 1. The system comprised a batch reactor to which two identical undivided flow-through electrolytic cells (parallel rectangular electrodes, 5.1 cm × 9.1 cm, interelectrode gap 3.0 mm, void volume 63 ml) were connected. The first electrolytic cell (Fe-sacrificial anode) (98.5% Fe) and Ti cathode was operated for Fe(II)/Fe(III) generation. The second electrolyzer (Cl$_2$-

Table 1
Operational parameters applied in the iron dissolution (sacrificial Fe anode) electrolysis experiments.

# exp.	pH_0	pH control	$[Cl^-]$ (mg/l)	Current density (mA/cm^2)	Voltage (V)	$[C_T^a]$ (mM)
1	2	√	0	10.77	2.01–1.98	0
2	5	√	0	10.77	3.56–3.27	0
3	5	–	200	10.77	3.27–2.89	6
4	5	√	200	10.77	3.25–2.87	6
5	6	–	200	10.77	3.24–3.16	6
6	6	√	200	10.77	3.48–3.15	6
7	6	√	200	10.77	2.46–3.79	25
8	6	√	200	2.16	1.46–1.11	6
9	6	√	200	5.39	2.09–1.77	6
10	6	√	200	21.55	5.18–4.82	6
11	6.5	√	200	10.77	3.52–3.41	6
12	7	√	200	10.77	3.59–3.58	6
13	6	√	1000	10.77	2.03–1.74	6
14	5	√	1000	10.77	1.98–1.71	6

^{a} C_T = total inorganic carbon concentration.

production cell) comprised of a Ti/RuO$_2$ anode and a Ti cathode was used to generate active chlorine for Fe(II) oxidation. A peristaltic pump (Masterflex®, 6–600 rpm) was used to recycle electrolyte (10 l) between the flow-through cells and the electrolyte holding vessel at a 1.72 l/min flow rate (resulting in a hydraulic retention time of 2.2 s). A magnetically stirred PVC reactor (height 40.5 cm, internal diameter 19.5 cm) was used as the electrolyte holding vessel. Two 0–5 A DC power supply devices (Prova 8000, M.R.C Ltd) were used to generate the required current. Temperature during the experiments was held constant at 19–21 °C.

Two independent experimental sets were conducted to separately quantify the Fe(II)/Fe(III)- and Cl$_2$ production rates in the two electrolysis systems, under varying operational conditions. Following the individual characterization, the two electrolyzers were operated together to define operational conditions for complete Fe(II) oxidation with the aim of providing an initial proof-of-concept to the new approach.

pH measurements and pH control were carried out using a specifically programmed automatic titration apparatus (Titrino 718, Metrohm, Switzerland). Constant pH (±0.03) was attained by 2.25 M H$_2$SO$_4$ addition. Ferrous iron concentration was determined using the modified phenanthroline method proposed by Herrera et al. [13]. Total iron concentration was measured by ICP (Optima 3000 DV, Perkin-Elmer). Ferric iron concentration was calculated by subtracting the ferrous iron concentration from the total iron concentration. Active chlorine concentration was determined by the DPD spectrophotometric method [14].

All reagents were of analytical grade. Appropriate amounts of sodium chloride (Frutarom Ltd, Israel) dried at 250 °C were dissolved in distilled water to maintain the required chloride ions concentrations. Sodium bicarbonate (Frutarom Ltd, Israel) reagent was added to the electrolyte solution shortly before the beginning of each experiment.

2.1. Iron anode dissolution experiments

The purpose of this set of experiments was to study the effects of electrolyte pH, buffering intensity of the electrolyte solution, applied current density and chloride ions concentration on the Fe(II) production efficiency and Fe(II) oxidation rate. Table 1 lists the operational parameters applied in the performed experiments. The second electrolyzer (hypochlorite production unit) was not operated in this experimental set. Generally, NaHCO$_3$ was added to the electrolyte to attain the required pH buffering capacity, apart from experiments #1 and #2 (Table 1) which were conducted with distilled water to which no bicarbonate was added. Na$_2$SO$_4$ was added to the electrolyte solution to establish electrical conductivity of ~1000 μS/cm. To remove possible iron oxide precipitates

from the iron anode surface the electrode was treated with sand paper and then polished by felt disk and washed with distilled water prior to each experiment. In all the experiments a charge of 900 C was transported through the cell (constant current mode), resulting in electrolysis periods of 15, 30, 60 and 150 min for experiments applied with currents of 1, 0.5, 0.25 and 0.1 A, respectively. The expected total iron concentration in the electrolyte solution (assuming 100% current efficiency) at the end of the experiments was 26.05 mg Fe/l. 5 ml electrolyte samples were taken at given intervals, acidified by 1 ml HCl 3M and analyzed for total, ferrous and ferric iron concentrations. To obtain the dissolved iron concentration the samples were syringe filtered (0.2 μm) (Sartorious Stedim Biotech, Germany).

2.2. Hypochlorite production experiments

Two sets of experiments were performed to estimate the effect of the chloride ion concentration and pH within the pH 4–6 range on the active chlorine production rates. First, active chlorine production rates were studied at chloride ion concentrations of 200, 400, 600, 800 and 1000 mg Cl/l in five different experiments (current density = 10.77 mA/cm^2, $[C_T]$ = 6 mM). Thereafter, the experiment was repeated at pH 4. In the combined process no active chlorine species accumulation was expected to occur due to their very rapid reaction kinetics with Fe(II) throughout the pH scale. Consequently, in this separate Cl$_2$-production experiment set only the initial active chlorine production rates were of the interest (once Cl$_2$ accumulates in the water the net rate of Cl$_2$ production decreases). 10 ml samples were taken periodically from the system and the active chlorine species concentration was determined without delay.

2.3. Simultaneous operation of sacrificial-iron and Ti/RuO$_2$ anode based electrolysis cells

Three experiments were conducted at various operational conditions. Current densities applied in the Cl$_2$-generation cell (Ti/RuO$_2$ anode) were calculated according to the expected Fe(II) production rate. Fe(II) species produced at the Fe-cell were expected to be oxidized in the bulk solution both by dissolved oxygen and active chlorine. For calculating the required current to be applied at the Cl$_2$-cell in order to achieve complete Fe(II) oxidation it was assumed that the overall Fe(II) oxidation rate is the sum of two results obtained from the individual electrolysis cells, irrespective of reciprocal effects. Another assumption was that the current efficiency for the active chlorine production is not a function of the applied current density. Table 2 lists the operational parameters applied in these tests.
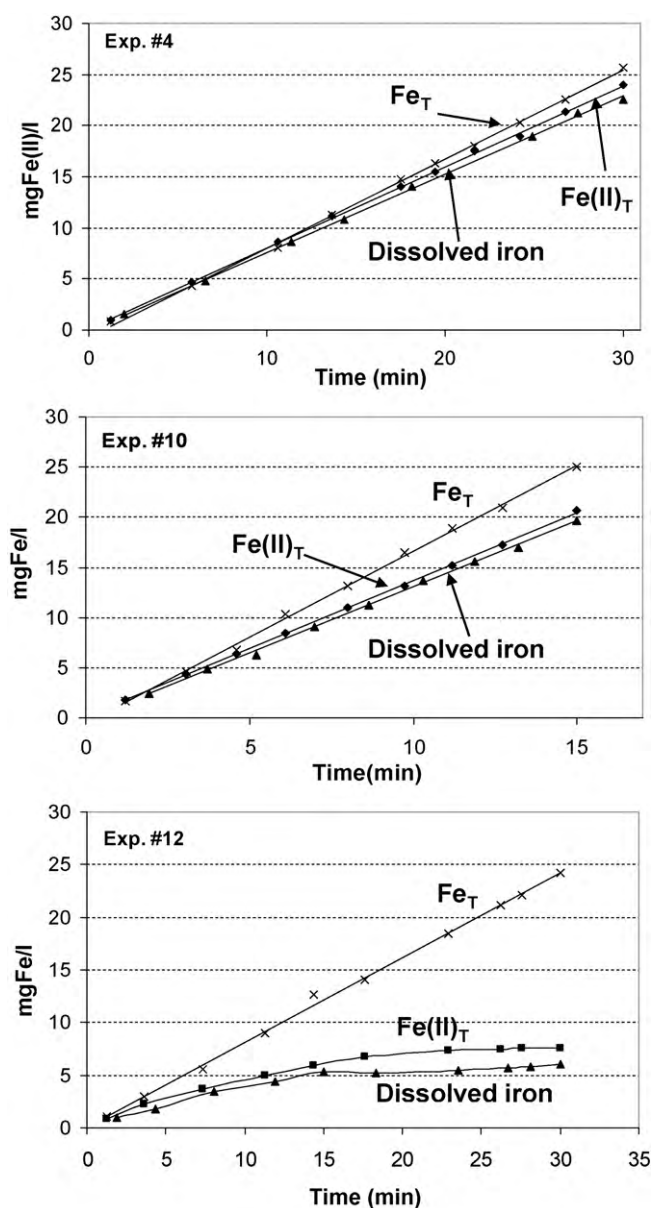
Table 2
Electrolyte composition, applied current density and resulting cell potentials in Cl_2- and Fe-cells simultaneous operation experiments.

# exp.	pH	[Cl⁻] (mg/l)	Fe-cell current density (mA/cm²)	Fe-cell voltage (V)	Cl₂-cell current density (mA/cm²)	Cl₂-cell voltage (V)
I	6.0	200	5.39	2.24–2.22	19.6	7.53–7.2
II	6.0	400	10.77	2.66–2.43	17.9	5.77–5.54
III	5.0	600	10.77	2.31–1.97	13.8	4.47–4.31

3. Results and discussion

3.1. Performance of the iron electrocoagulation cell

In all the experiments conducted with the Fe-electrolysis cell the dissolved Fe(II) concentration increased linearly with time ($R^2 > 0.998$) except for experiment #12 (pH 7, see Table 1) in which the Fe(II) concentration reached a plateau after 20–25 min (Fig. 2C). Fig. 2 shows results from experiments #10, #4 and #12 as examples for the data acquired in this experiment set. Fe(II) and Fe_T forma-
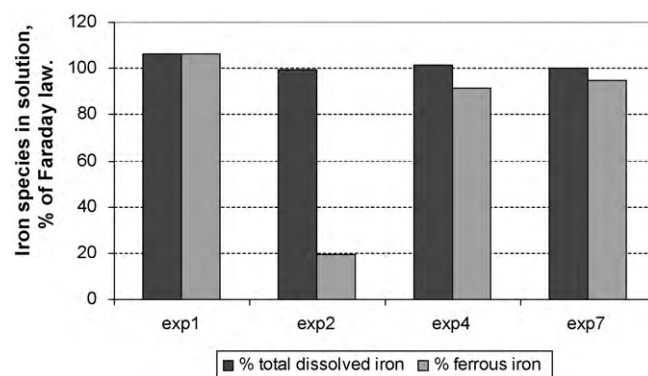

Fig. 2. Fe(II) and Fe(III) concentrations as a function of time in experiments #10, #4 and #12 (operational conditions listed in Table 1).

tion rates were obtained from the slope of the linear regression line (see Fig. 2). In experiment #12 the initial and final Fe(II) concentrations were used for calculating the oxidized Fe(II) fraction and the Fe(II) oxidation rate. The dissolution rate of the iron sacrificial anode was found to be in rough agreement with Faraday's low of electrolysis for all the experiments (96% < current efficiency for Fe dissolution < 106%). With respect to dissolution values observed to be above the theoretical 100% it is noted that higher rates of iron release than the theoretical values predicted by Faraday's low were observed in recent electrocoagulation studies. The common explanation for this phenomenon is chemical dissolution of the iron anode, accelerated at low-pH values [6] and high chloride ion concentrations [3]. The total dissolved iron concentrations (Fe_T) measured in the filtered samples were slightly lower (≤4%) than the measured Fe(II) concentrations in the experiments performed at $5 \le pH \le 6$. At pH 6.5 and pH 7 the differences were larger: 6.4% and 20.64%, respectively. This observation was attributed to complete ferric iron precipitation at pH > 5 coupled with absorption of Fe(II) species on the formed Fe(III) precipitates [15].

Increasing the Cl⁻ concentration from 200 to 1000 mg Cl/l in the experiments conducted at pH 6 (experiments #6 and #13, respectively) did not seem to significantly affect the Fe(II) oxidation rate: 83.7% and 81.6% of the dissolved iron remained in the Fe(II) form, respectively. Similar experiments were performed at pH 5 (experiments #4 and #14), again with no significant change in the Fe(II) oxidation rate (83.86% and 88.36% of the dissolved iron remaining in the Fe(II) form, respectively). Since the observed small difference in the Fe(II) oxidation rate could be attributed to normal analytical fluctuations it was concluded that the Cl⁻ concentration (strictly speaking, in the range 200 < Cl⁻ < 1000 mg/l) had very little effect on the Fe(II) oxidation rate.

The effect of the buffering intensity (β (M)) in the bulk solution on the Fe(II) oxidation rate is shown in Fig. 3, which presents the results obtained in experiments #1, #2, #4 and #7.

From Fig. 3 it can be concluded that when the Fe-anode electrolysis is carried out at pH ≤ 6 in buffered solutions (experiments #1, #4 and #7) more than 90% of the iron remains in the Fe(II) form. Note that in experiment #1 no external buffer was added but at pH

Fig. 3. Fe(II) and Fe(III) concentrations obtained in buffered and non-buffered experiments. Exp #1: pH 2.0 (constant), $I = 0.5$ A, no carbonate buffer ($\beta = 2.3 \times 10^{-2}$ M). Exp #2: pH 5 (constant), $I = 0.5$ A, no carbonate buffer ($\beta = 2.3 \times 10^{-5}$ M). Exp #4: pH 5 (constant), $I = 0.5$ A, $[C_T] = 6$ mM ($\beta = 6.13 \times 10^{-4}$ M). Exp #7: pH 6, $I = 0.5$ A, $[C_T] = 25$ mM ($\beta = 1.25 \times 10^{-2}$ M).
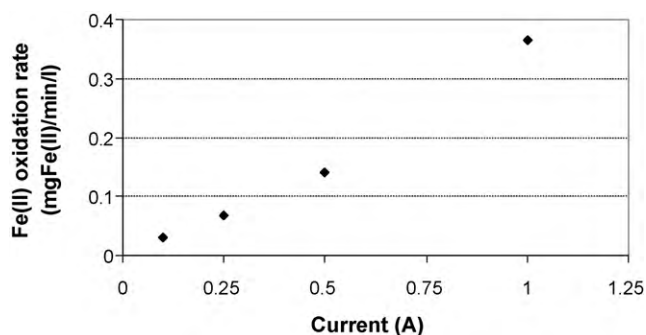
Fig. 4. Fe(II) oxidation rates as a function of the current applied in Fe-electrolytic cell (experimental conditions: pH 6.0; $[C_T]$ = 6 mM, $[Cl^-]$ = 200 mg/l).
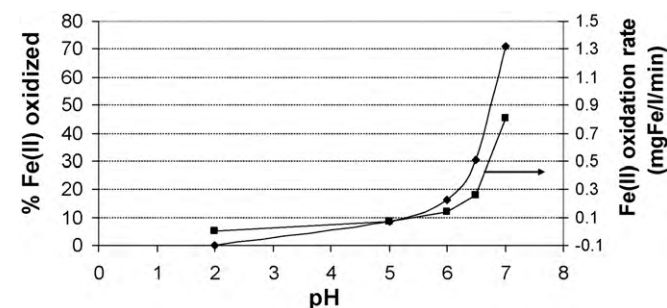

Fig. 5. Fe(II) to Fe(III) conversion rate and Fe(II) percentage of Fe$_T$ at the end of Fe-anode electrolysis experiments, as a function of electrolyte pH. Operational conditions: I = 0.5 A, $[Cl^-]$ = 200 mg/l, $[C_T]$ = 6 mM.

2 the solution is characterized by a natural buffering capacity of the H_2O system. Increasing C_T from 6 mM (common in natural water) to 25 mM had only a limited effect on the Fe(II) oxidation rate (90.1% vs. 94.5% of the total iron released from the anode remained in the Fe(II) form in experiments #6 and #7, respectively).

Fig. 4 shows the results obtained from experiments #6, #8, #9 and #10. These experiments were performed with different currents (0.5, 0.1, 0.25 and 1 A, respectively) while all the other operational parameters were maintained constant. In accordance with the results obtained by Lakshmanan et al. [5] the Fe(II) oxidation rate increased with an increase in the current density. The higher Fe(II) to Fe(III) conversion rates were consistent with the pH values that developed in the vicinity of the cathode due to the disappearance of H^+ ions via the reaction described in Eq. (3).

Fig. 5 shows the oxidation rates obtained in experiments #1, #4, #6, #11 and #12. Operational parameters were identical in all five experiments except for pH, which was maintained constant at pH 2, pH 5, pH 6, pH 6.5 and pH 7, respectively. To measure the overall change in pH as a result of the electrolysis reactions, two experiments were performed with no pH control and two initial pH values (experiment #3 at pH 5 and experiment #5 at pH 6). Gradual increase in the pH value of the electrolyte was observed in the two experiments and after 30 min the final pH values increased to 5.75 (experiment #3) and 6.32 (experiment #5). The Fe(II) oxidation rate recorded in experiment #3 (0.134 mg Fe^{2+}/l min) was significantly higher than the equivalent value obtained in experiment #4 (0.075 mg Fe^{2+}/l min), in which the operational parameters were similar but pH was maintained constant by the addition of concentrated H_2SO_4.

The Fe(II) oxidation rate observed in experiments #5 and #6 (controlled and uncontrolled initial pH 6, respectively) was almost identical (~0.14 mg Fe^{2+}/l min). This was attributed to a relatively small increase in pH in the uncontrolled experiment, probably due to the fact that electrolyte pH was close to 2nd pKa of the
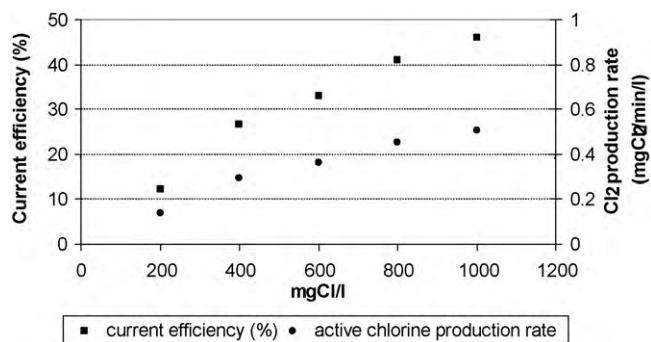

Fig. 6. Active chlorine production rate as a function of applied Cl^- concentration. Experimental conditions: pH 6.0 (constant), I = 0.5 A, $[C_T]$ = 6 mM.

carbonate system resulting in a relatively high buffering capacity.

### 3.2. Performance of the Cl$_2$ evolution electrolysis cell

The active chlorine concentration which generated by the operation of the Cl$_2$-cell was linear with time ($R^2 > 0.999$) (200 < $[Cl^-]$ < 1000 mg/l; experiment duration <15 min; results not shown). This allowed determining the relevant Cl$_2$ production rates by the slope of the linear regression curve. Fig. 6 shows the chlorine production rates as a function of the Cl^- concentration. Current efficiency for Cl$_2$ production (defined as the percentage of electrons used for actual Cl$_2$ production out of the applied current) increased from 12.4% at 200 mg Cl/l to 45.7% at 1000 mg Cl/l. Similar results (data not shown) were observed when the cell was operated at pH 4. It was concluded thus that within the ranges 4 < pH < 6 and 200 < Cl^- < 1000 Cl$_2$ production in the electrolytic cell was strongly affected by the Cl^- concentration but not affected by pH.

3.3. Simultaneous operation of the Fe- and Cl$_2$-electrolytic cells

Fig. 7 shows the overall production of Fe(III) species as a result of a simultaneous operation of the Fe- and Cl$_2$-production cells, as compared with the results obtained when the Fe-cell was operated alone at the same operational conditions.

As required, no Fe(II) concentration was observed as a result of the simultaneous operation of the Fe- and Cl$_2$-cells in experiment #I, i.e. all of the formed Fe(II) concentration was oxidized. The residual active chlorine concentration at the end of the experiment was also low, 0.15 mg Cl$_2$/l, indicating a very efficient combined operation of the two cells. The total Fe(III) concentration was somewhat higher than that predicted by Faraday's law (110.1% current efficiency), possibly due to enhancement of chemical iron anode oxidation by the active chlorine concentration in the water. Following Fe(OH)$_3$ precipitation, the final dissolved iron concentration was 0.031 mg Fe/l. During the experiment the pH of the solution increased from pH 6.0 to pH 6.19. The overall power consumption of the dual cell process was 23.35 kWh/kg Fe(III)$_{produced}$, out of which the relative demand of Cl$_2$-cell was 92.3% (taking into account the average experiment voltage and overall Fe(III) mass released by the anode).

Iron anode dissolution efficiency obtained in experiment #II (Fig. 7) was 99.0% of that predicted by Faraday's law. The final Fe(III) concentration was 23.44 mg Fe/l which amounted to 91.0% of the final total iron concentration. In the sole operation of the Fe-cell the corresponding value (similar operational conditions, 2nd electrolysis cell not operated) was 16.1%. No active chlorine was observed during and at the end of the operation. All the dissolved iron was present in the Fe(II) form. The power requirement of the dual-process was in this scenario 12.7 kWh/kg Fe(III)$_{produced}$, with
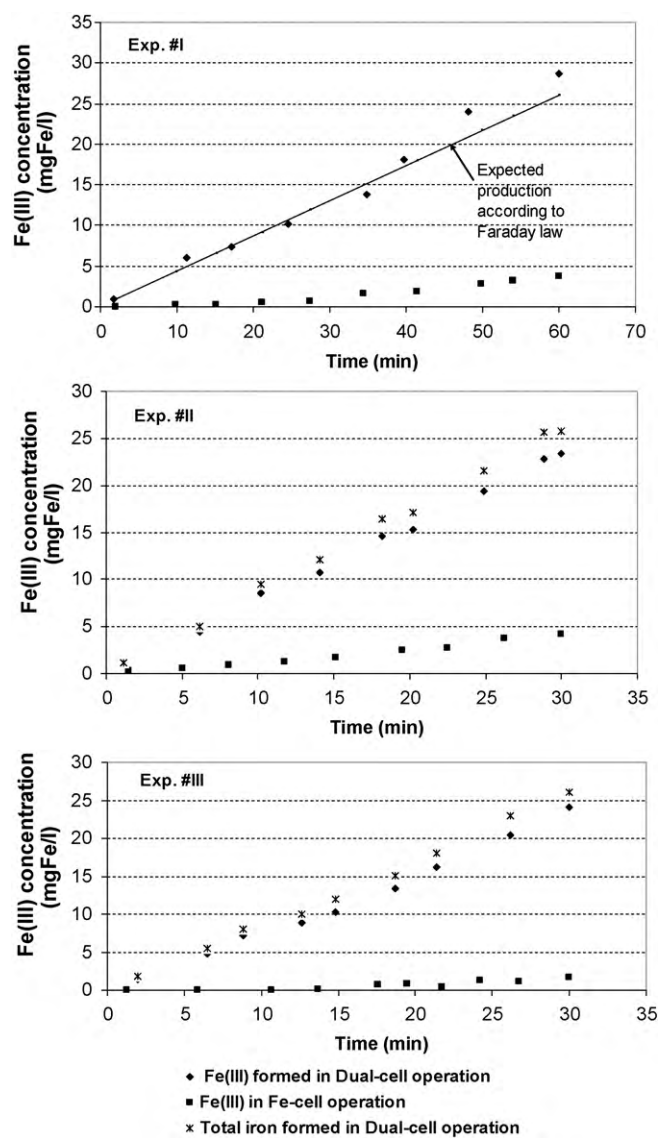
Fig. 7. Fe(III) concentration as a function of time in single Fe-cell operation vs. simultaneous Fe- and Cl_2-cell operation. Exp. #I: pH 6.0 (uncontrolled), $I_{Fe} = 0.25$ A, $I_{Cl_2} = 0.91$ A, $[C_T] = 6$ mM, $[Cl^-] = 200$ mg Cl/l. Exp. #II: pH 6.0 (uncontrolled), $I_{Fe} = 0.5$ A, $I_{Cl_2} = 0.83$ A, $[C_T] = 6$ mM, $[Cl^-] = 400$ mg Cl/l. Exp. #III: pH 5.0 (uncontrolled), $I_{Fe} = 0.5$ A, $I_{Cl_2} = 0.64$ A, $[C_T] = 6$ mM, $[Cl^-] = 600$ mg Cl/l.

78.6% of this energy being consumed by the Cl_2-cell. Based on the results it was concluded that a slight increase in the current density of the Cl_2-production cell would completely oxidize the remaining Fe(II) concentration. However, since the aim of this particular work was simply to prove the feasibility of the concept, no further experiments were performed.

In the 3rd combined test (experiment #III) the Fe dissolution current efficiency was 100.2%. Out of the total iron which was released from the Fe anode at the end of the run 92% were in the Fe(III) and 8% in the Fe(II) form. In the corresponding sole Fe-cell operation only 8.6% of the total iron was in the Fe(III) form and 91.4 in the Fe(II) form. No active chlorine was observed during and at the end of the experiment. At the conditions applied in experiment #III 8.07 kWh/kg Fe(III)$_{produced}$ were required, with 72.4% of this value attributed to the Fe(II) oxidation Cl_2-based cell. The final pH of the electrolyte solution in this scenario was 5.31. All the dissolved iron was in the Fe(II) form. As in the previous experiment, optimiza-

tion of the operation of the two cells to result in both Fe(II) = 0 and $Cl_2 \rightarrow 0$ was not carried out.

4. Conclusions

The product of iron anode dissolution in electrocoagulation systems is Fe(II). The rate at which the Fe(II) product is oxidized to the desired Fe(III) form is a function of solution pH and buffering capacity, the dissolved oxygen concentration and the applied electrical current density. Under certain conditions i.e. low dissolved oxygen concentration, pH < 6.5 and presence of a significant buffering capacity, the conversion rate from Fe(II) to Fe(III) is low, resulting in decreased efficiency of the electrocoagulation cell. This work has shown that complete Fe(II) oxidation can be achieved in such cases by the addition of a second Cl_2 production electrolysis cell that uses chloride ion concentrations normally present in water and wastewater. The results show that the higher the Cl^- concentration is, the more cost effective the process is, because of higher current efficiencies related to active chlorine production. Further work is required for optimizing the proposed dual-cell electrocoagulation method. A detailed kinetic study is required to determine Fe(II) oxidation rates at the cathode surface as a function of electrolyte characteristics and operational conditions. The effect of the Cl^- and active chlorine concentrations on the rate of the Fe anode dissolution also require further work. Power requirement of the proposed process was found to be lower at higher chloride ion concentrations due to higher current efficiency in the Cl_2-cell. Comparing the cost of supplying 1 kg of Fe(III) with conventional coagulation processes (i.e. dosage of ferric salts) it appears that the presented approach may be competitive above Cl^- concentrations of ~600 mg/l.

References

[1] A.A. Bukhari, Investigation of the electro-coagulation treatment process for the removal of total suspended solids and turbidity from municipal wastewater, Bioresour. Technol. 99 (2008) 914–921.
[2] Y.S. Yildiz, A.S. Koparal, S. Irdemez, B. Keskinler, Electrocoagulation of synthetically prepared waters containing high concentration of NOM using iron cast electrodes, J. Hazard. Mater. B139 (2007) 373–380.
[3] M.G. Arroyo, V. Perez-Herranz, M.T. Montanes, J. Garcia-Anton, J.L. Guinon, Effect of pH and chloride concentration on the removal of hexavalent chromium in batch electrocoagulation reactor, J. Hazard. Mater. 169 (2009) 1127–1133.
[4] H.A. Moreno, D.L. Cocke, J.A.G. Gomes, P. Morkovsky, J.R. Parga, E. Peterson, C. Garcia, Electrochemical reactions for electrocoagulation using iron electrodes, Ind. Eng. Chem. Res. 48 (2009) 2275–2282.
[5] D. Lakshmanan, D.A. Clifford, G. Samanta, Ferrous and ferric ion generation during iron electrocoagulation, Environ. Sci. Technol. 43 (2009) 3853–3859.
[6] M. Ben Sasson, W. Calmano, A. Adin, Iron-oxidation processes in an elctroflocculation (electrocoagulation) cell, J. Hazard. Mater. 171 (2009) 704–709.
[7] M. Yousuf, A. Mollah, R. Schennach, J.R. Parga, D.L. Cocke, Electrocoagulation (EC)-science and applications, J. Hazard. Mater. B84 (2001) 29–41.
[8] B. Morgan, O. Lahav, The effect of pH on the kinetics of spontaneous Fe(II) oxidation by O_2 in aqueous solution—basic principles and simple heuristic description, Chemosphere 11 (2007) 2080–2084.
[9] A. Khelifa, S. Moulay, F. Hannane, S. Benslimene, M. Hecini, Application of an experimental design method to study the performance of electrochlorination cells, Desalination 160 (2004) 91–98.
[10] C.W. Spalding, Reaction kinetics in the absorption of chlorine into aqueous media, AIChE J. 8 (5) (1962) 685–689.
[11] Y. Gendel, N. Levi, O. Lahav, $H_2S_{(g)}$ removal using a modified, low-pH liquid redox sulfur recovery (LRSR) process with electrochemical regeneration of the Fe catalyst couple, Environ. Sci. Technol. 43 (21) (2009) 8315–8319.
[12] G.H. Kelsall, Hypochlorite electro-generation. I. A parametric study of a parallel plate electrode cell, J. Appl. Electrochem. 14 (1984) 177–186.
[13] L. Herrera, P. Ruiz, J.C. Aguillon, A. Fehrmann, A new spectrophotometric method for the determination of ferrous iron in the presence of ferric iron, J. Chem. Tech. Biot. 44 (1989) 171–181.
[14] L.S. Clesceri, A.E. Greenberg, A.D. Eaton, Standard Methods for the Examination of Water and Wastewater, 20th ed., American Public Health Association/American Water Works Association/Water Environment Federation, Washington, DC, 1998.
[15] Y. Gendel, O. Lahav, Accurate determination of Fe(II) concentrations in presence of a very high soluble Fe(III) background, Appl. Geochem. 23 (2008) 2123–2129.